

Supplementary Information: Reduced Strain Mechanochemical Activation Onset in Microstructured Materials

Johanna J. Schwartz, Reza Behrou, Bo Cao, Morgan Bassford, Ariana Mendible, Courtney Shaeffer, Andrew J. Boydston*, and Nicholas Boechler*

Synthesis of pentenoyl-functionalized spiropyran

The pentenoyl-functionalized spiropyran was synthesized as described previously.[28] 4-pentenoyl anhydride was purchased from Sigma-Aldrich. The schematic of the final synthesis of the product is shown below.

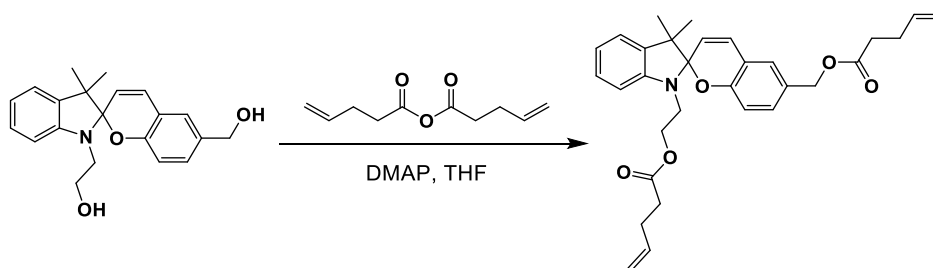


Figure S1. Schematic of pentenoyl-functionalized spiropyran.

Mold preparation for SP-PDMS

Acrylonitrile Butadiene Styrene (ABS) filaments were used for the melt material extrusion printing on a Flashforge Dreamer 3D Printer to print molds for SP-PDMS. The printing parameters were as follows: extruder temperature: 230 °C, platform temperature: 105 °C, base print speed: 60 mm/s, travel speed: 80mm/s, retraction length: 1.3 mm, retraction speed: 30 mm/s, fill density: 100%, fill pattern: hexagon, overlap perimeter: 15%, and cooling fan always on. Blue painter's tape was attached to the build platform prior to printing and wiped with ethanol prior to each print.

SP-PDMS polymerization

Pentenoyl-functionalized SP was added with P-60 base and curing agent together (base:curing agent = 20:1 w/w) and mechanically mixed. P-60 PDMS was purchased from Silicones, Inc.. The liquid PDMS prepolymer was then poured into the 3D printed molds and degassed at 35 Torr for 30 min by using a vacuum chamber until no bubbles were visible. Samples were then cured at 60 °C for 30 min. The PDMS sheets were peeled from the mold and outgrowth was removed with a razor blade.

Tensile testing for SP-PDMS samples

Tensile testing was conducted on an Instron 5585H load frame with a 50N load cell. Sample elongations were done at a rate of 7 mm/min, and pictures were taken using a Nikon X camera and an intervalometer. Spiropyran-PDMS samples were stretched to 70% or 200% elongation. After photographing the samples during elongation in which the blue higher-energy conformation of

activated SP-PDMS is visible, samples were kept in the load frame and tension was reduced to photograph the purple lower-energy conformation.

Synthesis and filamentation of PCL-spiropyran-PCL (SP-PCL)

Synthesis and filamentation process have been described previously.[29] Filamentation was done through Functionalize, Inc. to produce 10 kg of blended 1:9 SP-PCL: PCL filament in 1 kg spools. These spools were used for 3D printing.

Melt Material Extrusion of SP-PCL

Spiropyran-PCL objects were printed using a Flashforge Dreamer with the following settings: Extruder temperature 120 °C, platform temperature 40 °C, base print speed 20 mm/s, travel speed 50 mm/s, minimum speed 5 mm/s, first layer maximum speed 20 mm/s, first layer maximum travel speed 20 mm/s, maximum path overlap 30%, fill density 100%, overlap perimeter 30%, and cooling fan always on. Blue painter's tape was attached to the build platform prior to printing and wiped with ethanol prior to each print. Prints included ASTM D638 Type V dogbones, as well as square and triangular hole lattices.

Tensile testing for SP-PCL samples

Tensile testing was conducted on an Instron 5585H load frame with a 2 kN load cell. Sample elongations were done at a rate of 20 mm/min, and pictures were taken using a Nikon X camera and an intervalometer. Spiropyran-PCL samples were taken to 250% or 650% elongation. After photographing the samples during elongation in which the blue higher-energy conformation of activated SP-PCL is visible, samples were kept in the load frame and tension was reduced to photograph the purple lower-energy conformation.

Lighting setup and Camera settings

A CameraTrax 24 Color Card was used for white balancing prior to testing, and a Photogenic Light Kit with a softbox was used to create a uniform lighting environment. For SP-PCL samples, a white matte foam poster was placed behind the samples to make the background uniform. For SP-PDMS samples, a black poster board was used. For tensile testing of dogbones, the lighting was kept the same throughout testing for each sample. The lighting setup was modified slightly for tensile testing of lattices to deal with glare from the objects under tension, after which the lighting was kept the same throughout testing. Nikon camera settings: Shutter speed 1/15, F 7.1, ISO 400 (SP-PCL) or ISO 100 (SP-PDMS), exposure 0, evaluative metering on, image size Raw + F, flash exposure off. The intervalometer was set with a 4 or 3 second delay for SP-PCL or SP-PDMS samples, respectively, with pictures taken every 4 or 3 seconds.

Quantification of SP activation through tensile testing PCL dogbones

Immediately after elongation of the sample, it was relaxed while still in the grips of the load frame to its purple coloration. A photograph of this sample was taken. The sample was left in visible light for 24 hours to induce closing of the spiropyran. The sample was then placed in the same

lighting setup and grips, and an image of the reverted sample was taken. The elongated sample was then irradiated with UV from a broad-spectrum Mercury lamp for 5 min to achieve complete spiropyran activation. This UV activated sample was then placed back in the load frame grips, maintaining the same lighting conditions, and a picture was taken. Quantification and numerical analysis can be found in the supporting information.

Image Analysis

To extract local activation from an experimental image, an image processing algorithm was developed. In this algorithm, the following steps were performed on every image:

1. Adaptively (changing with grip extension) crop image to remove borders and consider central region of lattice.
2. Extract the red, blue, and green channels from the cropped images.
3. Remove the background by applying a threshold on the blue and green channels.
4. Compute the normalized color intensity I_{BG} as described in the main text.
5. Compute the local activation by scaling the averaged maximum intensity as described in the main text.

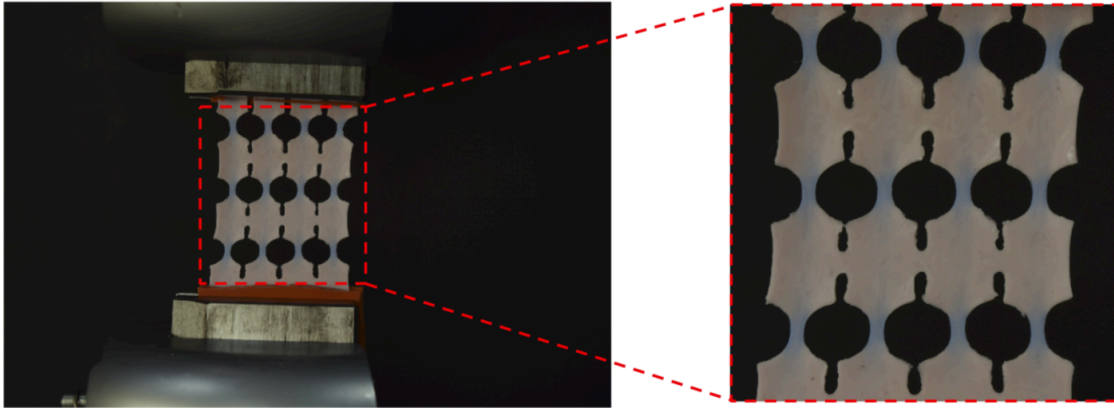


Figure S2. Schematic example of cropping of the original image in the image analysis.

Activation profiles

Applying the image processing algorithm to the dogbone samples, we extracted the activation profiles used in the numerical modeling. The extracted activation profiles were considered as the local activation, i.e. A_{actv} in Equation S1. A curve fitting algorithm was used to create smooth and differentiable activation profiles appropriate for the numerical modeling. For the SP-PDMS samples, the extracted local activation (shown in Figure S3) from the image analysis was considered as a function of the first strain invariant using the following fitting function:

$$A_{\text{actv}} = \alpha_1 \frac{\tanh(\beta_1 \eta_1) + \tanh(\beta_1 (I_1 - \eta_1))}{\tanh(\beta_1 \eta_1) + \tanh(\beta_1 (I_1^{\text{max}} - \eta_1))} + \alpha_2 \frac{\tanh(\beta_2 \eta_2) + \tanh(\beta_2 (I_1 - \eta_2))}{\tanh(\beta_2 \eta_2) + \tanh(\beta_2 (I_1^{\text{max}} - \eta_2))} + \alpha_3 \frac{\tanh(\beta_3 \eta_3) + \tanh(\beta_3 (I_1 - \eta_3))}{\tanh(\beta_3 \eta_3) + \tanh(\beta_3 (I_1^{\text{max}} - \eta_3))} \quad (3)$$

where I_1 is the first strain invariant. The other parameters extracted through the curve fitting are given as follows:

$$\alpha_1 = 1.4, \beta_1 = 5.0, \eta_1 = 0.0557, \alpha_2 = 6.0, \beta_2 = 5.3285, \eta_2 = 0.3, \alpha_3 = 27.6191, \beta_3 = 3.4783, \eta_3 = 1.4179, I_1^{max} = 10.0.$$

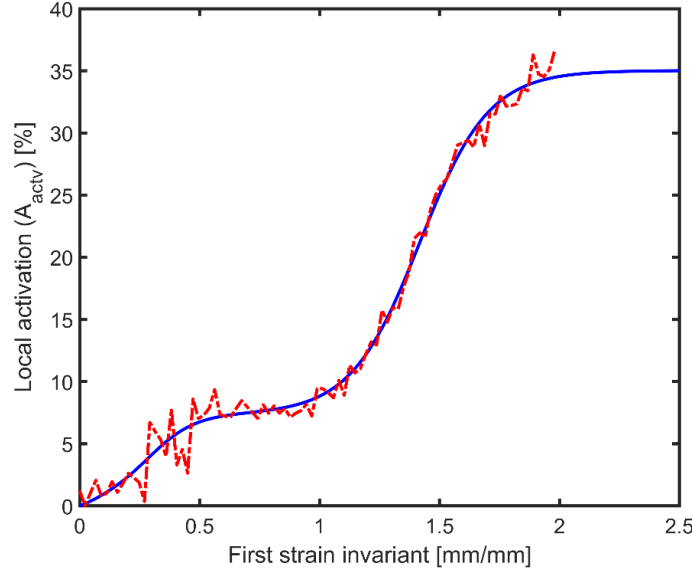


Figure S3. Local activation profile for the SP-PDMS samples. The dash-dot line corresponds to the experimental activation extracted from the image analysis and the solid line is the fitted analytical activation.

Similar to the SP-PDMS samples, we obtained the following local activation for the SP-PCL samples (see Figure S4), as a function of the first principal strain:

$$A_{actv} = \alpha_1 \frac{\tanh(\beta_1 \eta_1) + \tanh(\beta_1 (\epsilon_1 - \eta_1))}{\tanh(\beta_1 \eta_1) + \tanh(\beta_1 (\epsilon_1^{max} - \eta_1))} + \alpha_2 \frac{\tanh(\beta_2 \eta_2) + \tanh(\beta_2 (\epsilon_1 - \eta_2))}{\tanh(\beta_2 \eta_2) + \tanh(\beta_2 (\epsilon_1^{max} - \eta_2))} + \alpha_3 \frac{\tanh(\beta_3 \eta_3) + \tanh(\beta_3 (\epsilon_1 - \eta_3))}{\tanh(\beta_3 \eta_3) + \tanh(\beta_3 (\epsilon_1^{max} - \eta_3))} + \alpha_4 \frac{\tanh(\beta_4 \eta_4) + \tanh(\beta_4 (\epsilon_1 - \eta_4))}{\tanh(\beta_4 \eta_4) + \tanh(\beta_4 (\epsilon_1^{max} - \eta_4))}, \quad (4)$$

where ϵ_{max} is the first principal strain. The other extracted parameters are given as follows:

$$\alpha_1 = 4.0, \beta_1 = 9.60, \eta_1 = 0.0, \alpha_2 = 32.0, \beta_2 = 0.1573, \eta_2 = 20.97, \alpha_3 = 12.4276, \beta_3 = 0.547, \eta_3 = 29.0802, \alpha_4 = 12.0, \beta_4 = 0.2768, \eta_4 = 38.8001, \epsilon_1^{max} = 60.0.$$

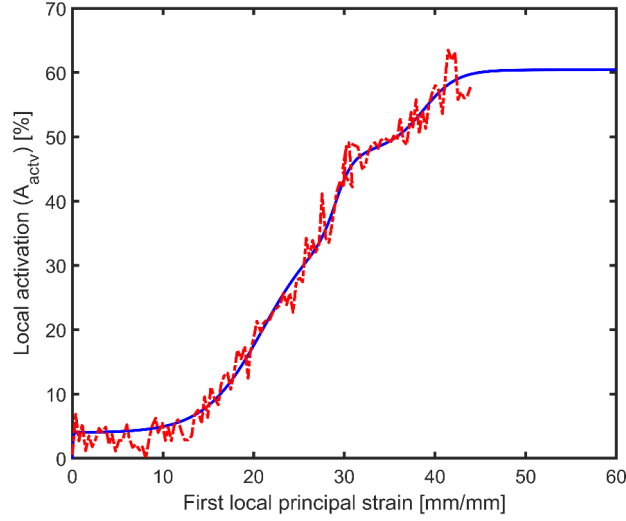


Figure S4. Local activation profile for the SP-PCL samples. The dash-dot line corresponds to the experimental activation extracted from the image analysis and the solid line is the fitted analytical activation.

Hyperelastic modeling of SP-PDMS

For numerical modeling of the SP-PDMS samples, finite strain hyperelasticity was considered. A nonlinear curving fitting algorithm was developed, considering different hyperelastic material models, to extract material parameters from uniaxial stress-strain tests of the dogbone samples (Figure S4). We used a Mooney-Rivlin hyperelastic material model. Under uniaxial loading conditions the uniaxial stress can be defined as follows using the Mooney-Rivlin material model:

$$P_{\text{uniaxial}} = 2(1 - \lambda^{-3})(\lambda C_{10} + 2C_{20}\lambda(I_1 - 3) + C_{11}\lambda(I_2 - 3) + C_{01} + 2C_{02}(I_2 - 3) + C_{11}(I_1 - 3)), \quad (5)$$

where λ is the principal uniaxial stretch, I_1 is the first strain invariant, and $C_{10} = 93212.2$ Pa, $C_{01} = 54825.7$ Pa, $C_{20} = -8829.4$ Pa, $C_{02} = 80464.9$ Pa, and $C_{11} = 83149.6$ Pa are material parameters. The Poisson's ratio, ν , was assumed to be equal to 0.49.

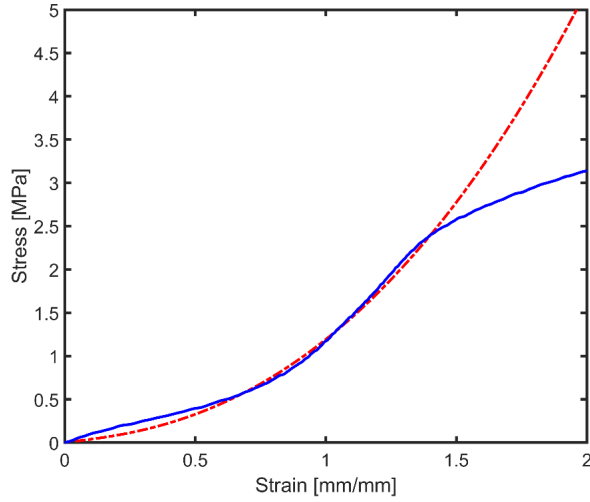


Figure S5. Stress-strain response of SP-PDMS dogbone sample. The solid line corresponds to the experimental stress-strain curve and the dash-dot line is the fitted analytical stress-strain curve based on the Mooney-Rivlin hyperelastic material model.

Elasto-plasticity modeling of SP-PCL

For numerical modeling of the SP-PCL samples, finite strain elasto-plasticity based on the von Mises yield surface was considered. To extract model and material properties from the uniaxial stress-strain curve, we first smoothed the original stress-strain curve using nonlinear curve fitting (see Figure S6). We assumed the proportional and elastic yield stress are the same. The smoothed engineering stress-strain curve was converted to the true stress-strain curve using the following approximations:

$$\varepsilon_{true} = \ln(1 + \varepsilon_{eng.}), \quad \sigma_{true} = \sigma_{eng.} e^{(\varepsilon_{true})}, \quad (6)$$

where $\varepsilon_{eng.}$ and $\sigma_{eng.}$ are the engineering strain and stress and ε_{true} and σ_{true} are the true strain and stress, respectively. The effective plastic strain was computed using the following steps:

1. Calculate the initial plastic strain, $\varepsilon_{int.}^p$, from the corresponding initial yield stress in the true stress-strain curve at which the initial yield occurs.
2. Compute the trial plastic strain, ε_{trial}^p , as follows:

$$\varepsilon_{trial}^p = \varepsilon^t - \varepsilon^e, \quad \varepsilon^e = \sigma_{true} / E, \quad (7)$$

where ε^t and ε^e are the total and elastic strain, respectively, and E is the Young's modulus extracted from the elastic portion of the engineering stress-strain curve.

3. Extract the effective plastic strain, ε^{ep} , by adjusting the trial plastic strain as follows:

$$\varepsilon^{ep} = \varepsilon_{trial}^p - \left(\varepsilon_{int.}^p - \frac{\varepsilon^{t_{yield}}}{E} \right), \quad (8)$$

where ε_{yield}^t is the initial yield strain. This adjustment is required to ensure that the effective plastic strain becomes zero when the total strain is equal to the initial yield strain. For numerical simulation purposes, a nonlinear curve fitting was used to smoothen the effective plastic strain function as shown in Figure S7.

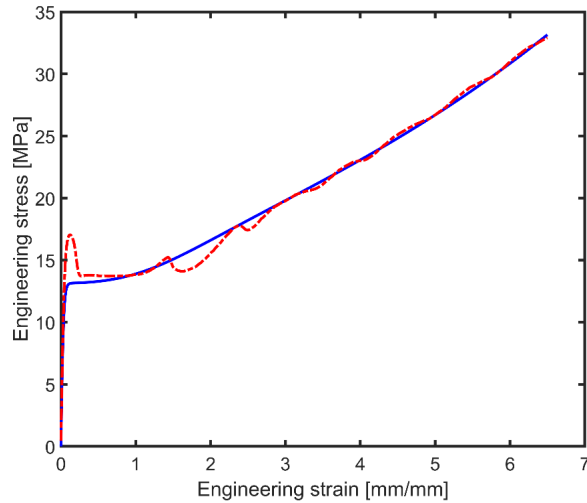


Figure S6. The original and fitted engineering stress-strain curve for the SP-PCL dogbone sample. The dash-dot line corresponds to the experimental stress-strain curve and the solid line is the fitted analytical stress-strain curve.

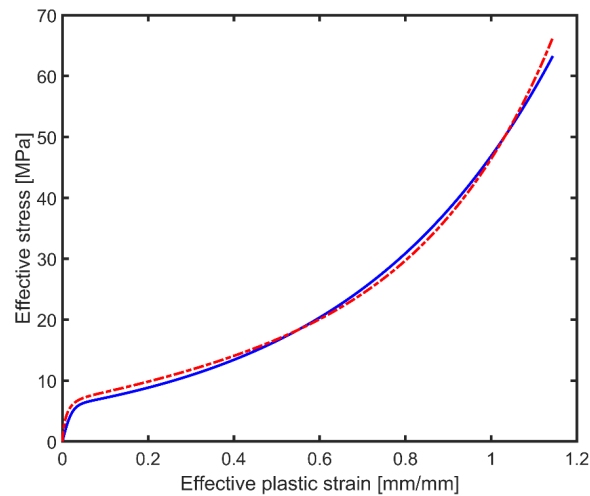


Figure S7. Extracted effective plastic strain function for the SP-PCL dogbone sample. The dash-dot line corresponds to the extracted effective stress – effective plastic strain curve and the solid line is the fitted analytical curve.

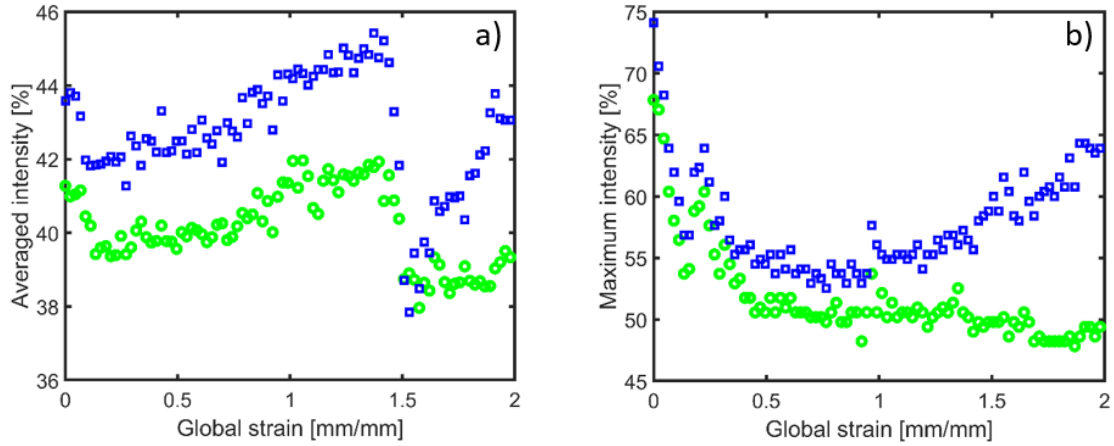


Figure S8. a) Averaged blue and green intensities during elongation of SP-PCL dogbone (the averaged largest 100 pixels in the measurement domain).
 b) Maximum blue and green intensities during elongation of SP-PCL dogbone. The green circle corresponds to $G/(R+G+B)$ and the blue square represents $B/(R+G+B)$.

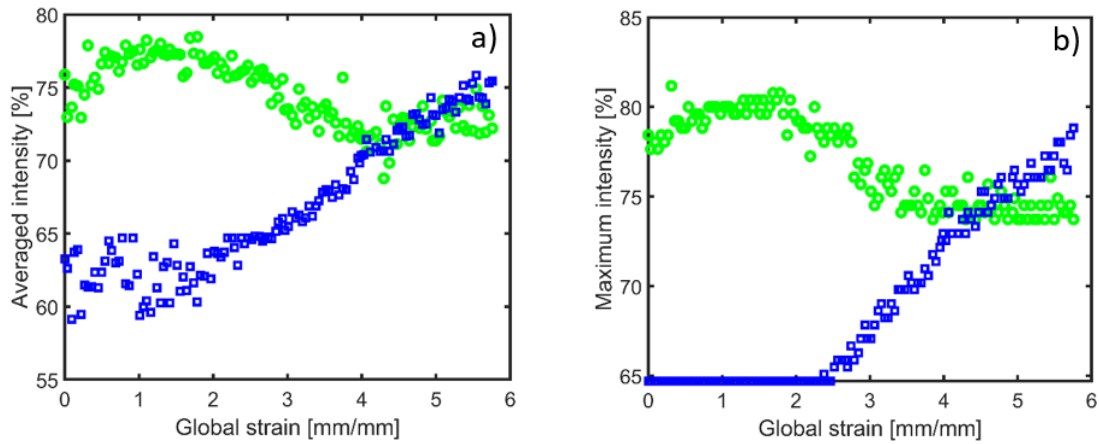


Figure S9. a) Averaged blue and green intensities during elongation of SP-PDMS dogbone (the averaged largest 100 pixels in the measurement domain).
 b) Maximum blue and green intensities during elongation of SP-PDMS dogbone. The green circle corresponds to $G/(R+G+B)$ and the blue square represents $B/(R+G+B)$.

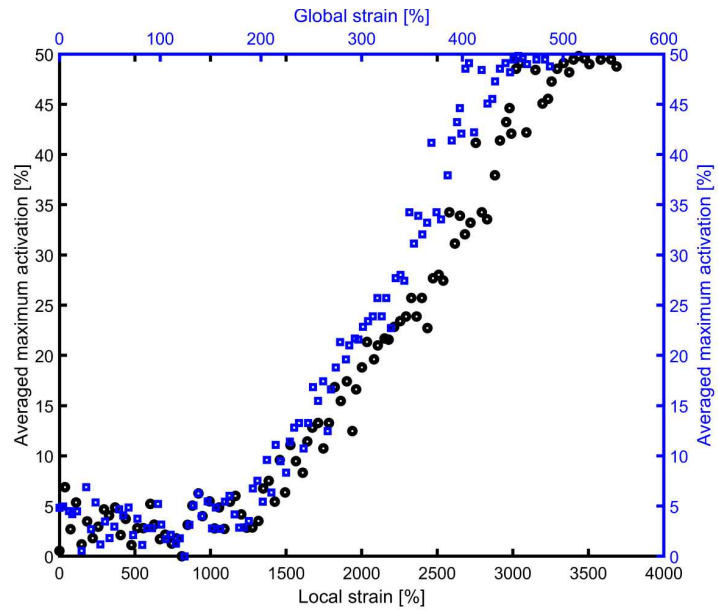


Figure S10. Comparison of local and global strain versus averaged maximum activation for the SP-PCL dogbone sample.



Figure S11. Lighting setup for taking images of the samples.

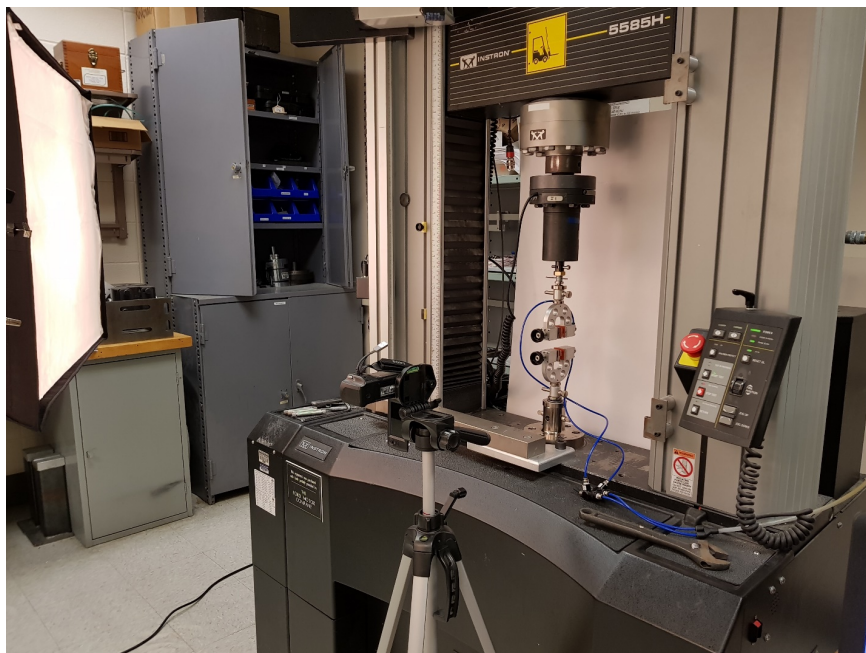


Figure S12. Camera setup (with lighting setup of S9) for taking images of SP-PCL samples (with white background). Nikon camera was used.



Figure S13. Camera setup (with lighting setup of S9) for taking images of SP-PDMS samples (with black background). Nikon camera was used.



Figure S14. Camera and lighting setup for taking images of SP-PDMS samples (with black background).

Movie S1. SP-PDMS dogbone tensile testing.

Movie S2. SP-PDMS lattice tensile testing.

Movie S3. SP-PCL dogbone tensile testing.

Movie S4. SP-PCL lattice tensile testing.